ELSEVIER

Materials Science and Engineering A337 (2002) 97–103

MATERIALS SCIENCE & ENGINEERING A

www.elsevier.com/locate/msea

On the evaluation of the ductility of thin films

J.M. Antunes [a], L.F. Menezes [b], M.F. Vieira [c], J.V. Fernandes [b,*], B. Trindade [d], A.S. Ramos [d], M.T. Vieira [d]

[a] Escola Superior de Tecnologia, Instituto Politécnico de Castelo Branco, Avenida do Empresário, P-6000 Castelo Branco, Portugal

[b] CEMUC, Departamento de Engenharia Mecânica, Faculdade de Ciências e Tecnologia, Polo 2 da Universidade de Coimbra, Pinhal de Marrocos, P-3030-201 Coimbra, Portugal

[c] GMM/IMAT, Departamento de Engenharia Metalúrgica e Materiais, Faculdade de Engenharia da Universidade do Porto, Rua Dr. Roberto Frias, P-4200-465 Porto, Portugal

[d] ICEMS, Departamento de Engenharia Mecânica, Faculdade de Ciências e Tecnologia, Polo 2 da Universidade de Coimbra, Pinhal de Marrocos, P-3030-201 Coimbra, Portugal

Received 26 July 2001; received in revised form 10 December 2001

Abstract

A new tensile test procedure has been developed to evaluate the ductility of thin films deposited on a substrate. The tensile sample has a continuously variable cross-sectional area, resulting in a continuous strain gradient along the sample after deformation. The films present cracks where the strain imposed exceeds their ductility. The strain attained at the boundary of the region where cracks appear characterises the film's ductility. This tensile test procedure has been used to evaluate the ductility of TiAl films deposited on an AISI 304 steel tensile sample. Cracks were observed by optical microscopy. The results of the evolution of the mean distance between cracks as a function of the deformation value are presented and discussed. A three-dimensional finite element code was used to simulate the deformation of this tensile sample. Special attention is devoted to the analysis of the state of stress and strain in the composite film/substrate. A similar study was made of a conventional tensile test sample to confirm and validate the results obtained from the modified sample. Moreover, the influence of the presence of cracks on the stress and strain distributions was also studied by numerical simulation. The experimental tests on conventional samples need to be interrupted at several strain values in order to follow the evolution of the cracks during the deformation. The ductility results obtained from conventional samples do not differ from those obtained with the modified sample. These conclusions and the simplicity of the method demonstrate the advantage of using the continuously variable cross-sectional area sample to study the ductility of thin films.

Keywords: Ductility; Numerical simulation; Thin films

1. Introduction

One important aspect of surface science and engineering is the production of films with particular mechanical properties, and the relationship between these properties and the performance of the composite. This is a difficult experimental task, which generally requires specialised experimental equipment. Various techniques have been proposed and used to evaluate the mechanical response of thin films. However, it is still difficult to evaluate the ductility of a film attached to a ductile substrate.

In this paper, we modified the geometry of the conventional tensile sample and proposed a new method to evaluate the mechanical response of thin films, by studying the evolution of the cracks in an approach similar to the technique called the periodic cracking method [1]. The modified tensile sample, which has a continuously variable cross-sectional area, was used to obtain a recognizable strain gradient along its gauge length after deformation. Experimentally, this is an easy way of determining the ductility of the film. It is possible to define, in the modified sample, the boundary of the region where cracks appear by using optical microscopy. This method has already been used to measure the

* Corresponding author. Tel.: +351-239-790-700; fax: +351-239-790-701

E-mail address: valdemar.fernandes@dem.uc.pt (J.V. Fernandes).

0921-5093/02/$ - see front matter
PII: S0921-5093(01)01991-8

ductility of TiAl thin films deposited onto AISI 304 stainless steel substrates [2,3].

The validation of such a method is an important objective of the present study. Numerical simulation can be a useful tool towards a better understanding of the mechanical behaviour of the composite film/substrate, if an adequate mechanical model has been formulated. In this study, a three-dimensional finite element code-EPIM3D, developed for the numerical simulation of large plastic deformation [4–6], is used to simulate the deformation of the modified tensile sample and to validate its applicability. Experimental and numerical studies on conventional tensile samples are compared with the new sample procedure to validate the latter.

2. New tensile test procedure

2.1. Sample and experimental results

A new tensile test procedure has been developed to evaluate the ductility of thin films. The tensile test is performed on a sample with a continuously variable cross-sectional area (Fig. 1), which allows to obtain a smooth strain gradient along its length, after deformation. The strain gradient in the sample is determined by measuring the mean deformation of fifteen regions along the sample (each one 4 mm long). The mean deformation in each region is determined by measuring the respective length, before and after the test, using a travelling microscope, with an accuracy of 1 μm.

The experimental results were obtained by performing tests on TiAl thin films deposited by d.c.-magnetron sputtering onto AISI 304 stainless steel substrates, as described elsewhere [2,3]. The sample geometry is such that when plastic deformation sets in ($\varepsilon \approx 0.01$) at the maximum cross-sectional area, the strain in the minimum cross-sectional area is approximately equal to the limit of the homogeneous plastic strain of the stainless steel substrate ($\varepsilon \approx 0.40$). However, to ensure accuracy in the evaluation of the relatively low ductility of most ceramic films, the tensile test must be performed under conditions where the deformation is less than $\varepsilon = 0.10$ in the minimum cross-sectional area. As a consequence, the maximum cross-sectional area of the sample is still in the elastic domain. After this deformation, the boundary of the region where cracks appear in the film can be determined using optical microscopy. The strain attained in this boundary region characterises the film's ductility.

The linear strains in the TiAl films along the tensile axis of the sample, for a displacement of $\Delta u = 5$ mm, is shown in Fig. 2. Analysis of the results presented in this figure shows that, as expected, the deformation increases with a decrease in the cross-sectional area. It can also be seen that the TiAl film has a ductility close to $\varepsilon = 0.02$ (strain value attained in the boundary region where cracks appear). This value is similar to those obtained in conventional tensile tests performed at room temperature (see for example [7–9]). The cracks appear, initially in the normal direction to the tensile axis and, in the case of larger deformations, at 45° to the tensile axis, as shown in Fig. 3. In this figure, three different regions of the sample are displayed (A, B, and C as in Fig. 2). In Fig. 2, only distances between cracks normal to the symmetry axis were measured.

Fig. 4 shows the evolution with deformation of the maximum, mean and minimum distances between cracks. For $\varepsilon < 0.05$ crack spacing decreases as the strain increases. For $\varepsilon > 0.05$ the mean crack spacing between cracks normal to the axis of the sample becomes constant. The crack spacing approaches constant values close to 48, 27 and 16 μm, for the maximum, mean and minimum crack distances, respectively. Other authors [1,10–12] report a similar distribution of crack spacing with deformation in the case of brittle films deposited onto ductile substrates.

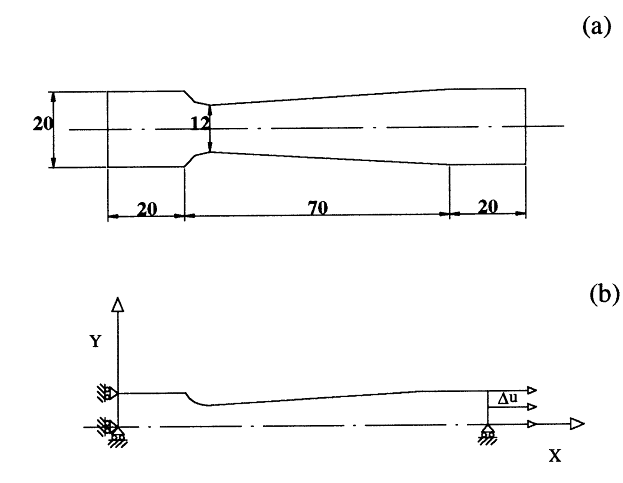

Fig. 1. Continuously variable cross-sectional area sample; (a) tensile test sample (dimensions in mm), (b) boundary conditions.

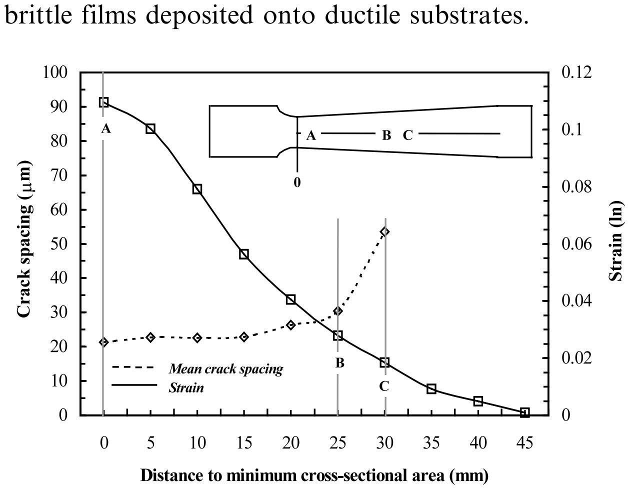

Fig. 2. Experimental results showing the evolution of strain and crack spacing in TiAl films along the axis of the modified sample.

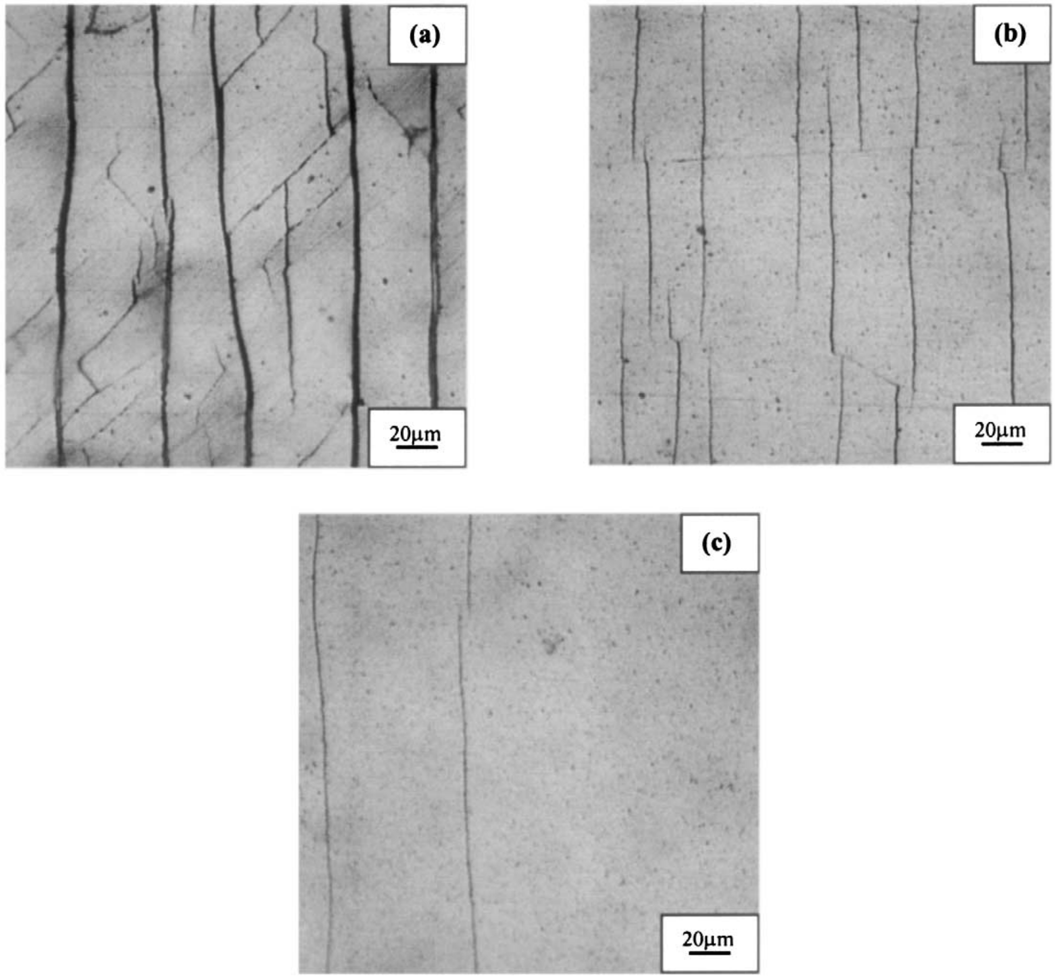

Fig. 3. Optical micrographs showing cracks in the TiAl films at different strain values, for region A, B and C of Fig. 2, respectively: (a) $\varepsilon = 0.11$; (b) $\varepsilon = 0.03$ and (c) $\varepsilon = 0.02$.

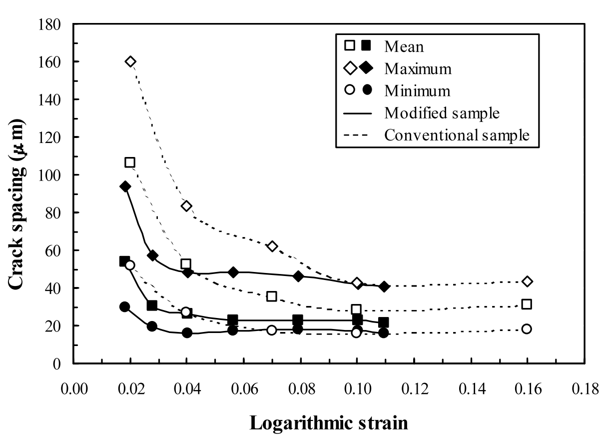

Fig. 4. Example of the evolution of the mean, maximum and minimum crack spacing with deformation, for modified tensile samples. The evolution of the mean, maximum and minimum crack spacing with deformation for conventional tensile samples is also shown. Experimental results obtained in TiAl films deposited onto stainless steel substrates. Only distances between cracks normal to the symmetry axis were measured.

2.2. Numerical validation

The mathematical formulation associated with the elastoplastic behaviour of the material and with the mechanical model [4] is briefly described below. Hooke's isotropic law is used to describe the elastic strains involved in the process. The model takes into account large elastoplastic strains and rotations. It uses the von Mises yield criterion and an associated plastic flow rule with isotropic work-hardening behaviour described by the Swift law: $\bar{\sigma} = K(\varepsilon_0 + \bar{\varepsilon}^{\mathrm{p}})^n$, where $\bar{\sigma}$ and $\bar{\varepsilon}^{\mathrm{p}}$ are the equivalent stress and plastic strain. K, n and ε_0 are constants for a particular material ($\sigma_0 = K(\varepsilon_0)^n$) is the material yield stress), as determined in classical tensile tests. This mechanical model was implemented in code EPIM3D which uses an implicit time integration operator.

The tensile test simulations were performed on samples of stainless steel sheets, 2 mm thick, coated with 4 μm thin film. The mechanical properties of both materials, substrate and film, are presented in Table 1.

Table 1
Material constants used in the numerical simulation (Swift law parameters: K, n and ε_0; yield stress, σ_0, Young's modulus, E, and Poisson's ratio, ν)

Properties	Substrate	Film 1	Film 2	Film 3	Film 4
σ_0 (MPa)	300	1000	5000	30 000	30 000
K (MPa)	1330	1280	5500	–	–
n	0.35	0.10	0.05	–	–
ε_0	0.009	0.083	0.149	–	–
E (GPa)	200	180	180	180	700
ν	0.33	0.25	0.25	0.25	0.25

Films 3 and 4 do not deform plastically, so the constants σ_0, K, n and ε_0 have no values.

In this table, the mechanical properties of the substrate correspond to the stainless steel sheets used in the experimental tests. Two types of film were used in this study. Their mechanical properties are given in Table 1 (films 1 and 2). The mechanical properties of the experimental case studied above (TiAl film) is somewhere between these two films. Films 3 and 4 were only used for the study described in the next paragraph concerning the influence of the mechanical properties of the film on the stress distribution in conventional tensile samples in the presence of cracks.

The sample geometry used in the simulations is the same as in the experimental tests (Fig. 1(a)). Due to the symmetry along the tensile axis only half of the sample is used in the numerical simulations. A schematic representation of the boundary conditions is presented in the same figure (Fig. 1(b)). The finite element mesh of this sample is composed of a 785 eight-node isoparametric hexahedra, made up of three layers, one for the film and two for the substrate.

The main objective in the numerical simulations performed on the sample with a variable cross-sectional area is to check, whether or not this kind of sample is adequate for the study of the ductility of thin films. For all the tests whose results are shown below, a displacement $\Delta u = 5$ mm was applied. It should be noted that all the simulations are accurate up to the onset of the first crack in the film. In fact, no rupture criterion is used in the simulations. The first conclusion from the calculation is that the state of stress at each point in the sample with the particular geometry under study is similar to the simple tension specimen. The study of redundant stress components (other than σ_{xx}) shows that these are very small in the gauge length of the sample. An example of shear stress τ_{xy} distribution for the composite film 1/substrate is shown in Fig. 5(a). Fig. 5(b) shows the equivalent stress distribution for the same composite.

The influence of the presence of the substrate on the behaviour of the film was also analysed. Examples of the numerical results are shown in Fig. 6(a) and (b). These figures show equivalent strain distribution, at the same displacement ($\Delta u = 5$ mm), for the bulk substrate material and for the composite (film 1/substrate), respectively. It can be concluded that no major differences exist in the equivalent strain, in both cases. Moreover, the plastic strain profile does not show any discontinuity when crossing from the film to the substrate (Fig. 6(b)). This means that the presence of the substrate under the film does not modify its strain conditions.

3. Conventional tensile tests

3.1. Experimental results

Tensile test experiments were also performed on 4 μm TiAl thin films deposited on stainless steel tensile samples of conventional geometry (Fig. 7(a)). The tensile test was interrupted to allow the microscopic observation of the morphology of the cracks, at successively increasing strain values. The amount of strain in each case was measured with a video extensometer.

The results for the evolution of crack spacing with strain are presented in Fig. 4. Analysis of this figure shows that in general the behaviour is the same as that presented of the continuously variable cross-sectional area tensile sample. The ductility is approximately $\varepsilon = 0.02$ (strain value at which the first crack is observed) and the maximum, mean and minimum crack spacing stabilises at values close to 43, 30 and 17 μm, respectively. As mentioned above, for the variable cross-sectional area tensile sample the ductility is also approximately $\varepsilon = 0.02$ and the crack spacing approaches constant values close to 48, 27 and 16 μm, for the maximum, mean and minimum distances, respectively. This crack spacing stabilisation occurs for strain values close to $\varepsilon = 0.05$. These results confirm that the new test procedure using a continuously variable cross-sectional area is adequate to describe the evolution with plastic strain of the film crack distribution.

3.2. Numerical simulations

Simulations of conventional tensile tests were performed on a composite film/substrate, for which the

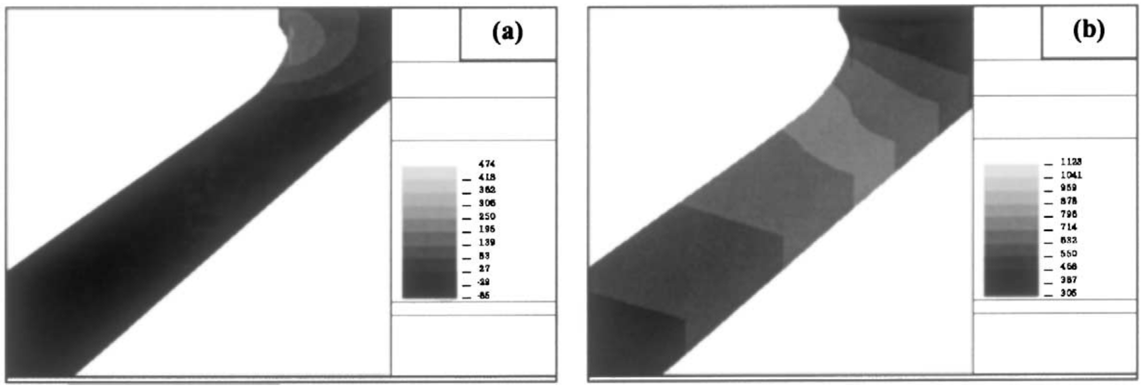

Fig. 5. Distribution at the end of the simulation ($\Delta u = 5$ mm) of the: (a) shear stress τ_{xy} (MPa) and (b) equivalent stress (MPa), for the composite film 1/substrate.

respective mechanical properties are shown in Table 1. The examples presented in this table allow us to perform a parametrical study of the effect of yield stress and Young's modulus on the stress distribution in the film. The mechanical properties of films 1 and 2 bordered the experimental case of TiAl in the present study, the results of which are shown in Figs. 2–4. Due to the high yield stress σ_0, films 3 and 4 do not attain plastic deformation under the displacements applied in this study.

As in the case of variable cross-section samples, the conventional samples are achieved using a 2 mm thick substrate coated with a 4 μm thin film. Only 1/4 of the sample was used in the simulation because of the symmetry along the tensile axis. A schematic representation of the boundary conditions is presented in Fig. 7(b). In order to analyse the behaviour of the composite film/substrate in the presence of cracks, several small plates of film with lengths, L, were studied ($L = 20$, 80 and 200 μm, Fig. 7(b)). With these different lengths of film plate, we intend to simulate different distances between two adjacent cracks. The finite element mesh of the sample is composed of eight-node isoparametric hexahedra, where the minimum number of elements is 3390 ($L = 20$ μm) and the maximum number is 6090 ($L = 200$ μm), made up of four layers, two for the film and two for the substrate.

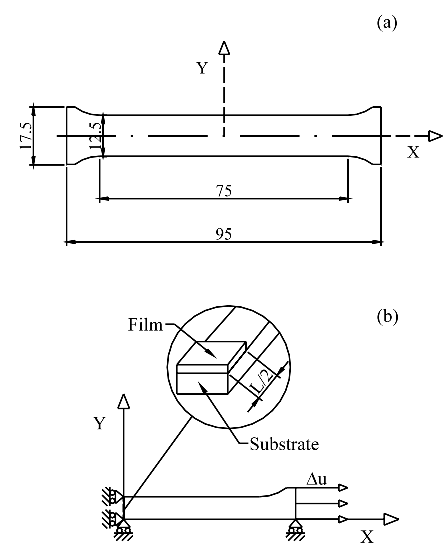

Fig. 7. Conventional tensile test sample used in the simulations with a thin film: (a) sample geometry (dimensions in mm); (b) boundary conditions for the numerical sample and details of film plate in the central region of the sample.

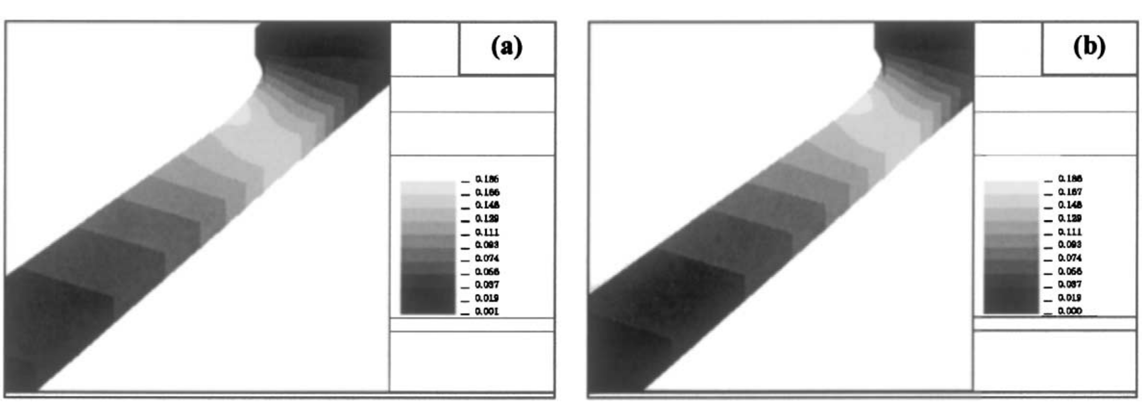

Fig. 6. Equivalent strain distribution at the end of the simulation ($\Delta u = 5$ mm) for the (a) substrate material and (b) composite film 1/substrate.

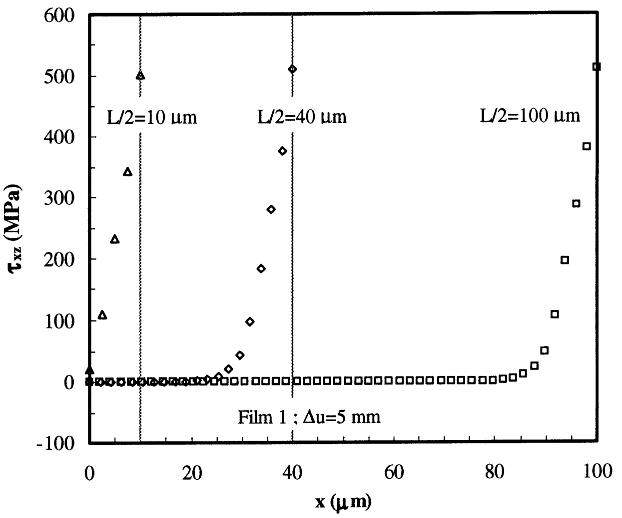

Fig. 8. Shear stress, τ_{xz}, distribution along the interface between film 1 and the substrate, for the three lengths of film ($L = 20$, 80 and 200 μm and $\Delta u = 5$ mm).

For all the tests, displacements of $\Delta u = 2$, 3.5 and 5 mm (corresponding to strain values of approximately $\varepsilon = 0.05$, 0.09 and 0.13, respectively) were applied. Fig. 8 shows the shear stress distribution along the interface between film 1 and the substrate, for the three lengths of film. The distribution of the shear stress τ_{xz} is similar for all cases, τ_{xz} is zero in the central region and dramatically increases close to the edge of the film. The increase is fairly similar for all the film lengths. The corresponding distribution of the tensile mean stress σ_{xx} is shown in Fig. 9. The stress σ_{xx} tends to attain the same stable maximum value for all lengths of film and decreases near the edge of the film, following identical profiles in all cases. The length of the region where σ_{xx} decreases is

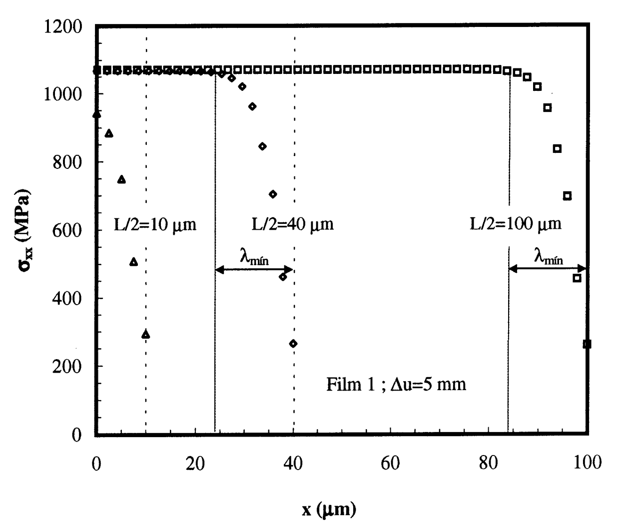

Fig. 9. Tensile mean stress, σ_{xx}, distribution along the interface between film 1 and the substrate, for the three lengths of film ($L = 20$, 80 and 200 μm and $\Delta u = 5$ mm).

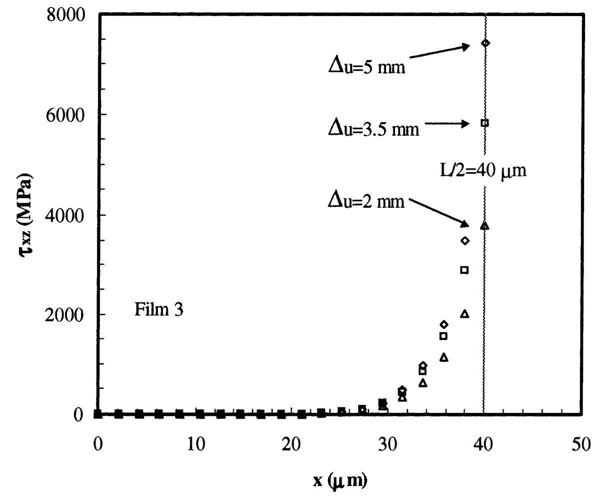

Fig. 10. Shear stress, τ_{xz}, distribution along the interface between film 3 and the substrate, for the three displacements used in this study ($\Delta u = 2$, 3.5 and 5 mm and $L = 80$ μm).

named $\lambda_{\min}$ and its value is about 17 μm. This can be observed in Fig. 9, where $L = 80$ and 200 μm.

The influence of the degree of deformation and the mechanical behaviour of the film on the shear and tensile stress distribution was also analysed. Examples are shown in Figs. 10 and 11. The profile of these stresses near the edge of the film is such that the value of $\lambda_{\min}$ does not change during deformation and does not depend on the properties of the film. The value $\lambda_{\min} = 17$ μm coincides with the experimental results, where the minimum distance between cracks in TiAl films is close to 15 μm. The experimental results indicated a value close to 40 μm for the maximum distance between the cracks, which is similar to that obtained by numerical simulation: $\lambda_{\max} = 2\lambda_{\min} = 34$ μm.

The tensile stress $\sigma_{xx}(x)$, which can cause fracture in the film, is coupled with the shear stress $\tau_{xz}(x)$ at the interface through an integral equation [10]:

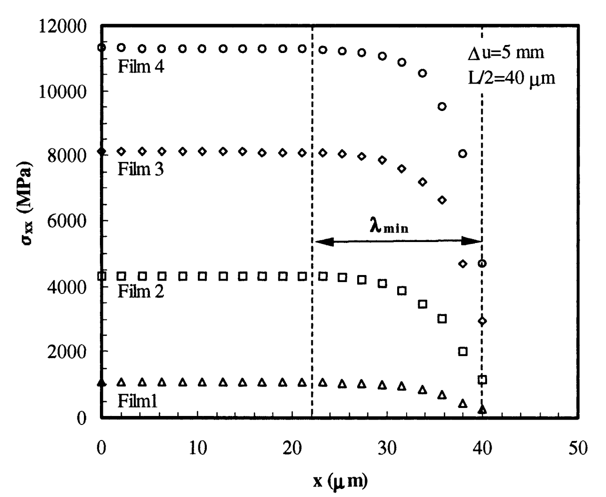

Fig. 11. Tensile mean stress, σ_{xx}, distribution along the interface film/substrate for the four film materials used ($L = 80$ μm and $\Delta u = 5$ mm).

$$\sigma_{xx}(x) = \left(\frac{1}{\delta}\right) \int_{L/2}^{x} \tau_{xz}(x)\,\mathrm{d}x \quad (1)$$

where δ is the film thickness and x is the co-ordinate along the interface with origin at the crack. From this equation, the maximum shear stress, $\tau_{\max}$, at the edge of the interface can be obtained as a function of the stress σ_{f}:

$$\tau_{\max} = \frac{k\delta\sigma_{\mathrm{f}}}{\lambda_{\max}} \quad (2)$$

where $\lambda_{\max}$ is the maximum crack spacing in the film and the constant k depends on the shear stress distribution along the interface. $\tau_{\max}$ represents the lower limit of the adhesion between the film and the substrate, if decohesion does not occur. k was determined using Eq. (2), for each case of substrate/film in Table 1 and for each one of the three strain values. The results show that k does not depend on the strain value. However, k does depend on the mechanical properties of the film: $k = 3.9$, 4.9, 7.5 and 7.8, respectively, for films 1–4. In the literature [10], it is possible to find k with values equal to 2, π and 6, obtained from analytical models, which do not consider the mechanical properties of the film.

4. Conclusions

In this study, a new tensile test procedure is proposed to evaluate the ductility of brittle thin films deposited on a ductile substrate. The tensile sample has a continuously variable cross-sectional area. The method has been applied successfully to characterise the ductility of TiAl films deposited on AISI 304 stainless steel. The advantage of the new sample test procedure lies in its simplicity. Numerical simulations also confirm that the method adequately describes the mechanical response of thin films.

Acknowledgements

The authors are indebted to the Fundação para a Ciência e Tecnologia do Ministério da Ciência e Tecnologia and the Praxis Program XXI, for financial support.

References

[1] D.C. Agrawal, R. Raj, Acta Metall. 37 (1989) 1265.
[2] M.T. Vieira, B. Trindade, A.S. Ramos, J.V. Fernandes, M.F. Vieira, Thin Solid Films 343 (1999) 43.
[3] C. Coelho, A.S. Ramos, B. Trindade, M.T. Vieira, J.V. Fernandes, M.F. Vieira, Surf. Coat Technol. 120 (1999) 297.
[4] L.F. Menezes, J.V. Fernandes, D.M. Rodrigues, Mat. Sci. Eng. A 264 (1999) 130.
[5] J.M. Antunes, L.F. Menezes, J.V. Fernandes, in: J.A. Covas (Ed.), Material Forming: Experimental Investigations, Physical Approaches, Numerical Modelling and Engineering Cases, Proceedings of the second ESAFORM Conference, Guimarães-Portugal, 1999, p. 183.
[6] J.M. Antunes, L.F. Menezes, J.V. Fernandes, M.F. Vieira, B. Trindade, A.S. Ramos, M.T. Vieira, in: A.S. Khan, H. Zhang, Y. Yuan (Eds.), Plasticity and its Current Applications, Proceedings of the 8th International Symposium: PLASTICITY 2000, Whistler Resort, Canada, 2000, p. 463.
[7] V. Recina, B. Karlsson, Mater. Sci. Technol. 15 (1999) 57.
[8] M. Fu, Y. Hong, Y. Ma, S. Li, J. Mater. Sci. 35 (2000) 4937.
[9] M. Yamaguchi, H. Inui, K. Ito, Acta Mater. 48 (2000) 307.
[10] F.S. Shieu, R. Raj, S.L. Sass, Acta Metall. 38 (1990) 2215.
[11] M.S. Hu, A.G. Evans, Acta Metall. 37 (1989) 917.
[12] F.S. Shieu, M.H. Shiao, Thin Solid Films 306 (1997) 124.